COMMUNICATION

ChemComm
www.rsc.org/chemcomm

Multicomponent redox gradients on photoactive electrode surfaces†

Dirk M. Guldi,*[a] Israel Zilbermann,[a] Greg Anderson,[a] Andrew Li,[a] Domenico Balbinot,[b] Norbert Jux,*[b] Maria Hatzimarinaki,[b] Andreas Hirsch*[b] and Maurizio Prato*[c]

[a] *Radiation Laboratory, University of Notre Dame, Notre Dame, IN 46556, USA*
[b] *Institut für Organische Chemie, Universität Erlangen-Nürnberg, Henkestr. 42, 91054 Erlangen, Germany*
[c] *Dipartimento di Scienze Farmaceutiche, Università di Trieste, Italy*

Received (in Cambridge, UK) 7th January 2004, Accepted 27th January 2004
First published as an Advance Article on the web 18th February 2004

Redox gradients have been used to tailor the arrangement of photoactive ITO-electrodes at the molecular level.

When irradiated with suitable photon energy, alternate layers of donor and acceptor chromophores can give rise to interlayer electron transfer. If the charge separation between layers is efficient, and the charges can be driven to the electrodes, the ensemble will work as a photovoltaic device.[1] Critical issues in the development of this technology are an easy way of self-assembling the components and the creation of the correct redox gradients to direct the photocurrent in the desired way.[2] Electrostatically-driven deposition of oppositely charged components offers the great advantage of packing the building blocks individually.[3] In addition, this supramolecular technique allows a greater control over the organization and increased flexibility in replacing individual building blocks. In the present communication, we describe a new molecular assembly, where multipurpose energy/redox gradients within a series of chromophores are essential in helping *i)* to attain good absorption coverage of the solar spectrum, *ii)* to funnel solar light unidirectionally to an active core, *iii)* to separate charges within that active core, and *iv)* to transport electrons and holes in opposite directions. We demonstrate that the optimized interplay within sequence *i) – iv)* leads to efficiencies of photon to current conversion of up to 1.6%, for a novel ITO construct that contains only *4 molecular layers*.

Scheme 1 shows the electro- and photoactive components employed in this work.[4] Common to all the building blocks is their water-solubility at pH 7. By cyclic voltammetry in water, increasing oxidation strength was found among the electron donors – Fc^{1+} (E_{ox} = +0.62 V) < ZnP^{8-} (E_{ox} = +0.77 V) < H_2P^{8+} (E_{ox} = +0.94 V) *versus* SCE. The one-electron oxidation of D-C_{60}^{9-} falls out of our potential window of +1.5 V. On the cathodic side, only the D-C_{60}^{9-} reduction occurs at −0.7 V *versus* SCE. As a reference point, the conduction band of ITO is around −0.25 V *versus* SCE.[5] Among the singlet excited state energies the following trend emerges: Fc^{1+} (> 2.5 eV)[6a] > ZnP^{8-} (2.1 eV)[6b] > H_2P^{8+} (1.9 eV)[6b] > D-C_{60}^{9-} (1.78 eV).[6c] Taking the redox potentials and excited state energies in concert an ITO · D-C_{60}^{9-} · H_2P^{8+} · ZnP^{8-} · Fc^{1+} arrangement (Scheme 2) appears to be most profitable for attaining the most efficient flow of *i)* excited state energy, *ii)* holes and *iii)* electrons.

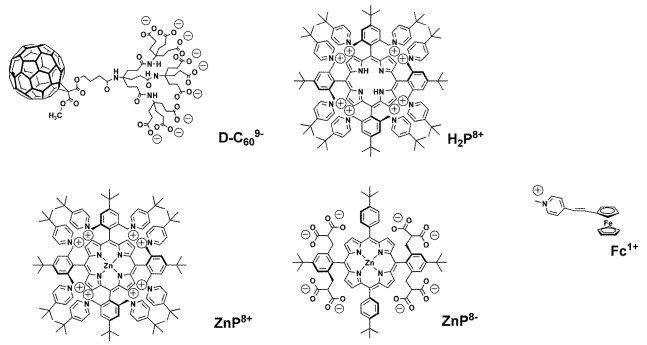

Scheme 1

The hydrophobic glass and quartz slides were coated with a **p**oly(**d**iallyl**d**imethyl**a**mmonium chloride) (PDDA) base layer (drafted as · in Scheme 2). Such a modified surface carries a maximum density of positively charged ammonium groups, which assist in anchoring and spatially fixing negatively charged moieties, such as D-C_{60}^{9-}. Once a D-C_{60}^{9-} monolayer is absorbed at the PDDA surface, strong van der Waals interactions between C_{60} cores facilitate a double layer formation, leaving the anionic dendrimer branches on the surface. In the next step the octacationic ZnP^{8+} or H_2P^{8+} building blocks were deposited *via* electrostatic interactions with the anionic dendrimer branches in a strict monolayer fashion. Subsequent layers were built up analogously utilizing cationic/anionic contacts.

Conditions for all the individual deposition steps were optimized by monitoring *i)* the absorption spectra on modified glass substrates and *ii)* AFM images on covered silicon wafers. The objective was to obtain a closely packed surface coverage with a maximum absorption cross section throughout the solar spectrum. This goal was achieved by immersing the substrates for time intervals of *ca.* 45 min into the aqueous stock solutions (~ 10 μM).[7] Representative absorption spectra for PDDA/D-C_{60}^{9-}, PDDA/D-C_{60}^{9-}/H_2P^{8+}, PDDA/D-C_{60}^{9-}/H_2P^{8+}/ZnP^{8-} and PDDA/D-C_{60}^{9-}/H_2P^{8+}/ZnP^{8-}/Fc^{1+} are summarized in Fig. S1, where the broadening of the absorption cross-section in the visible region enhances the light harvesting performance.

AFM images were routinely taken to test the surface structure. Fig. S2 shows 5 μm × 5 μm and 1 μm × 1 μm images of PDDA/D-C_{60}^{9-}, PDDA/D-C_{60}^{9-}/H_2P^{8+}, PDDA/D-C_{60}^{9-}/H_2P^{8+}/ZnP^{8-} and PDDA/D-C_{60}^{9-}/H_2P^{8+}/ZnP^{8-}/Fc^{1+}. For PDDA the structureless and rough features characteristic of assemblies of polyelectrolyte materials are observed. Completely different images were obtained after the subsequent coverage with D-C_{60}^{9-}. Typically, fine-grained images, although not resolved down to the molecular level, were found with 2D-aggregates of 20–50 nm sizes. Under optimized deposition conditions close packing is achieved, leading to a continuous uniform film. Shorter immersions lead to much less packed surfaces with large voids between the 2D-aggregates.

Photocurrents of the modified ITO electrodes were measured in oxygen-free conditions with 1 mM ascorbate/0.1 M NaH_2PO_4 and a Pt counter electrode. The selected composition guarantees that the electrical circuit remains closed: the primary function of ascorbate is to reinstate the oxidized building block (*i.e.*, H_2P^{8+}, ZnP^{8-} and

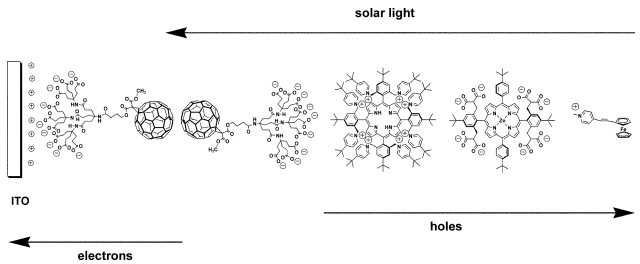

Scheme 2

† Electronic supplementary information (ESI) available: experimental section. See http://www.rsc.org/suppdata/cc/b4/b400027g/

DOI: 10.1039/b400027g

Fc^{1+}), while the reduced building block (*i.e.*, D-C_{60}^{9-}) transfers the electrons to the electrode.

Generally, the photoaction spectra of the different composites show good resemblances with their absorption characteristics – see Fig. 1. The simplest system, namely, PDDA/ D-C_{60}^{9-} shows broad and featureless responses with only a notable intensification in the blue region (*i.e.*, < 450 nm), where C_{60} absorbs most strongly. From the monochromatic light response we calculate a photon to current conversion efficiency (IPCE) of 0.01%, while just PDDA yields 0.001%.

Ensembles that integrate ZnP and/or H_2P building blocks show much stronger responses throughout the visible. In particular, both Soret-regions – centered around 425 nm – and Q-band regions – centered around 575 nm – clearly identify the two porphyrin chromophores as the major photoactive species.[8] Relative to the PDDA/D-C_{60}^{9-} system, the IPCE values for PDDA/D-C_{60}^{9-}/H_2P^{8+} (0.08%) and PDDA/D-C_{60}^{9-}/ZnP^{8+} (0.15%) reflect a 7- and 13-fold amplification, respectively. Also, the IPCE value determined for PDDA/D-C_{60}^{9-}/ZnP^{8+} is higher than previous reports for PDDA/ZnP-C_{60} (*i.e.*, 2.5 times)[9a] and PDDA/PSS/C_{60}-NiP (*i.e.*, 4.8 times),[9b] where electron donor and electron acceptor are covalently linked to each other.

If the order of deposition of the components is inverted, the efficiency decreases. An H_2P^{8+}/D-C_{60}^{9-} construct, instead of D-C_{60}^{9-}/H_2P^{8+}, showed a 5-fold drop in photocurrent. This is due to the mismatches in the individual redox steps: instead of an electron injection evolving from $C_{60}^{\bullet-}$, the photocurrent mechanism must change to hole injection from the oxidized $H_2P^{\bullet+}$. To confirm this assumption and to overcome the resulting effects, we applied an electrical bias to either accelerate or decelerate the charge injection into ITO. For D-C_{60}^{9-}/H_2P^{8+}, going in 200 mV intervals from +200 mV to −400 mV, a gradual photocurrent decrease up to 54% is noted. This decrease reflects the fact that, parallel with the bias, the energy gap for $C_{60}^{\bullet-} \rightarrow ITO_{electron}$ is reduced and the flow of charges is suppressed. For H_2P^{8+}/D-C_{60}^{9-}, under the same conditions, 35% higher photocurrents are generated, suggesting that $H_2P^{\bullet+} \rightarrow ITO_{hole}$ becomes more and more exothermic. In a different experiment, we compared aerobic and anaerobic conditions and found differences only for H_2P^{8+}/D-C_{60}^{9-}, which maximized at a 20% photocurrent loss.[10] In conclusion, photoexcitation of the porphyrin chromophores is succeeded by the formation of $C_{60}^{\bullet-}$/$H_2P^{\bullet+}$ or $C_{60}^{\bullet-}$/$ZnP^{\bullet+}$. From the reduced acceptor (*i.e.*, $C_{60}^{\bullet-}$) the electrons flow exothermically to the ITO conduction band. The oxidized donors (*i.e.*, $H_2P^{\bullet+}$ or $ZnP^{\bullet+}$), on the other hand, are reduced at the solid/liquid interface by ascorbate.

Comparing now the more complex PDDA/D-C_{60}^{9-}/H_2P^{8+}/$ZnP^{8-}$and PDDA/D-C_{60}^{9-}/H_2P^{8+}/ZnP^{8-}/Fc^{1+} with the simple PDDA/D-C_{60}^{9-}/H_2P^{8+}, we see a 14-fold and 20-fold enhancement of the photocurrent, respectively. This corresponds to high IPCE values of 1.0% and 1.6%. Three major changes impact the mechanistic consideration. Firstly, the new ZnP^{8-} and Fc^{1+} building blocks further enhance the absorption coverage of the solar spectrum. Secondly, both of them pass on their excited state energies unidirectionally to H_2P^{8+} or D-C_{60}^{9-}. Thirdly, once $C_{60}^{\bullet-}$/$H_2P^{\bullet+}$ is formed, the electrons and holes shift in different directions – ITO still collects the electrons, while the holes transfer step-by-step to ZnP^{8-} and Fc^{1+}.

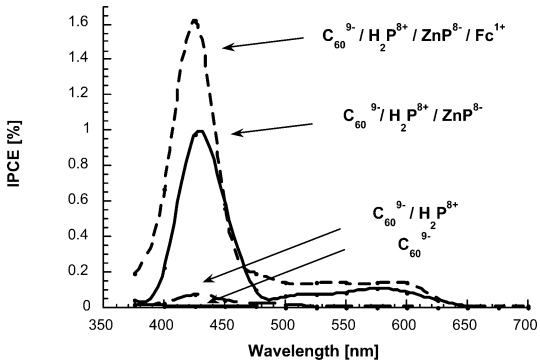

Fig. 1 Photoaction spectrum of photoactive ITO-electrodes covered with D-C_{60}^{9-}, H_2P^{8+}, ZnP^{8-}, Fc^{1+} as electro- and photoactive components under deoxygenated and short circuit conditions – see legend for details.

A novel concept is presented for tailoring the arrangement of photoactive ITO-electrodes at the molecular level. The current approach differs from the layer-by-layer strategy, where sandwich layers of covalently linked donor–acceptor dyads were integrated between layers of polyelectrolytes, but affording small IPCEs.[8,9] Following the controlled deposition of D-C_{60}^{9-}, H_2P^{8+}, ZnP^{8-}, Fc^{1} building blocks – utilizing electrostatic and van der Waals interactions – ITO-electrodes were modified that showed remarkable IPCEs of up to 1.6%. Relative to the simplest systems (*i.e.*, PDDA/ D-C_{60}^{9-}), this corresponds to a 108-fold performance improvement. Experiments are in progress to implement the new gradient control to a higher number of layers.

This work was supported by the Office of Basic Energy Sciences of the US Department of Energy (NDRL No. 4511), Deutsche Forschungsgemeinschaft (SFB 583), University of Trieste, MIUR (PRIN 2002, prot. 2002032171), and EU (RTNs: WONDERFULL and FAMOUS). I.Z. acknowledges his sabbatical leave from the Nuclear Research Centre Negev, Beer Sheva, Israel.

Notes and references

1 (*a*) E. W. McFarland and J. Tang, *Nature*, 2003, **421**, 616; (*b*) W. U. Huynh, J. J. Dittmer and A. P. Alivisatos, *Science*, 2002, **295**, 2425; (*c*) M. Gratzel, *Nature*, 2001, **414**, 338; (*d*) L. Schmidt-Mende, A. Fechtenkotter, K. Mullen, E. Moons, R. H. Friend and J. D. MacKenzie, *Science*, 2001, **293**, 1119; (*e*) A. Shah, P. Torres, R. Tscharner, N. Wyrsch and H. Keppner, *Science*, 1999, **285**, 692.

2 See for example: B. A. Gregg, *J. Phys. Chem. B*, 2003, **107**, 4688.

3 (*a*) G. Decher and J. D. Hong, *Ber. Bunsen-Ges. Phys. Chem.*, 1991, **95**, 1430; (*b*) M. Ferreira, J. H. Cheung and M. F. Rubner, *Thin Solid Films*, 1994, **244**, 806; (*c*) S. W. Keller, H. N. Kim and T. E. Mallouk, *J. Am. Chem. Soc.*, 1994, **116**, 8817; (*d*) Y. Lvov, G. Decher, H. Haas, H. Mohwald and A. Kalachev, *Physica B*, 1994, **198**, 89; (*e*) N. A. Kotov, J. H. Fendler and I. Dekany, *J. Phys. Chem.*, 1995, **99**, 13065.

4 (*a*) For D-C_{60}^{9-} see M. Braun, S. Atalick, D. M. Guldi, H. Lanig, M. Brettreich, S. Burghardt, M. Hatzimarinaki, E. Ravanelli, M. Prato, R. van Eldik and A. Hirsch, *Chem. Eur. J.*, 2003, **9**, 3867; (*b*) for ZnP^{8+}, ZnP^{8-}, H_2P^{8+} see N. Jux, *Org. Lett.*, 2000, **2**, 2129 and SI 1 (*c*) Fc^{1+} is commercial *trans*-4-[2-(1-ferrocenyl)vinyl]-1-methylpyridinium iodide.

5 F. Fromherz and W. Arden, *J. Am. Chem. Soc.*, 1980, **102**, 6211.

6 (*a*) Y. S. Sohn, D. N. Hendrickson and H. B. Gray, *J. Am. Chem. Soc.*, 1971, **93**, 3603; (*b*) D. M. Guldi and N. Jux, unpublished data; (*c*) D. M. Guldi and M. Prato, *Acc. Chem. Res.*, 2000, **33**, 695.

7 For experimental conditions see supporting information.

8 (*a*) Fluorescence experiments indicate the almost quantitative electron transfer quenching (factor is ~ 80) of the porphyrin fluorescence in D-C_{60}^{9-}/H_2P^{8+} and C_{60}^{9-}/ZnP^{8+} relative to H_2P^{8+} and ZnP^{8+} (*b*) see also H. Yamada, H. Imahori, Y. Nishimura, I. Yamazaki, T. K. Ahn, S. K. Kim, D. Kim and S. Fukuzumi, *J. Am. Chem. Soc.*, 2003, **125**, 9129.

9 (*a*) I. Zilbermann, G. A. Anderson, D. M. Guldi, H. Yamada, H. Imahori and S. Fukuzumi, *J. Porphyrins Phthalocyanines*, 2003, **7**, 357; (*b*) D. M. Guldi, I. Zilbermann, G. A. Anderson, K. Kordatos, M. Prato, R. Tafuro and L. Valli, *J. Mater. Chem.*, 2004, **14**, 303; (*c*) D. M. Guldi, C. Luo, D. Koktysh, N. A. Kotov, T. Da Ros, S. Bosi and M. Prato, *Nano Lett.*, 2002, **2**, 775.

10 O_2, as an electron carrier, accepts electrons from $C_{60}^{\bullet-}$, which are located at the surface (*i.e.*, $H_2P^{\bullet+}$/$C_{60}^{\bullet-}$), while in $C_{60}^{\bullet-}$/$H_2P^{\bullet+}$ $C_{60}^{\bullet-}$ are *i)*, hard to access and *ii)*, undergo rapid charge shift to ITO.